The bicyclo[2.1.1]hexan-2-one system: a new probe for the experimental and computational study of electronic effects in π-facial selectivity in nucleophilic additions

Goverdhan Mehta,[a,*] S. Robindro Singh,[a] Vanessa Gagliardini,[a] U. Deva Priyakumar[b] and G. Narahari Sastry[b,*]

[a]*Department of Organic Chemistry, Indian Institute of Science, Bangalore 560 012, India*
[b]*Department of Chemistry, Pondicherry University, Pondicherry 605 014, India*

Abstract—The remotely substituted 5-*exo*-bicyclo[2.1.1]hexan-2-one system is introduced as a new probe to study long range electronic effects on π-face selectivity during hydride reduction and a systematic computational study demonstrates good predictability at the semi-empirical level.

Prediction and control of stereoselectivities during nucleophilic additions to the carbonyl group is a fundamental issue in stereogenesis. While the role of steric effects in controlling π-face selection during addition to the carbonyl group is well recognized and predictable, the precise nature and effectiveness of long range electronic effects in determining π-face selectivity is a matter of ongoing inquiry and debate.[1] Examples are now known where remote electronic effects can overwhelm steric effects and there is the possibility of such effects finding applications in stereoselective syntheses.[2] In order to separate steric and electronic effects, several probe systems, wherein the two faces of the carbonyl group are in an isosteric environment, have been introduced.[3] We have reported that in *endo* substituted bicyclo[2.2.1]heptan-7-ones **1**[3a,b] and bicyclo[2.2.2]-octan-2-ones **2**,[3c] 4-substituted-9-norsnoutanone **3**[3d] and related systems, where the carbonyl group is in a sterically neutral disposition, distal substituents can influence stereochemical outcome (*syn*- versus *anti*-addition) in a profound way. Continuing our investigations in the area,[1b,3a–e] we now introduce 5-*exo*-substituted-bicyclo[2.1.1]hexan-2-ones **4** as a new probe system to explore further the role of distal electronic modifications on π-face selectivity. We have also employed the experimental results on **4** to test the predictability of various computational models at different levels of theory.

In light of our interesting observations during the hydride reduction of **1**–**3**, π-face selection studies with **4** were a natural impulse. Besides the broad structural resemblance to **1** and **2** and isosteric environment around the carbonyl group as revealed by high level calculations, the skeleton of **4** has some distinctive features. The substituent in **4** is farther removed from the stereoinduction center compared to **1** and the electronic effects are transmitted through the connecting cyclobutane bonds. Further, the carbonyl group is in the 'off' position from the vertical plane in which the substituent resides. Thus, a study of face selection in a range of derivatives of **4** was of intrinsic interest. How-

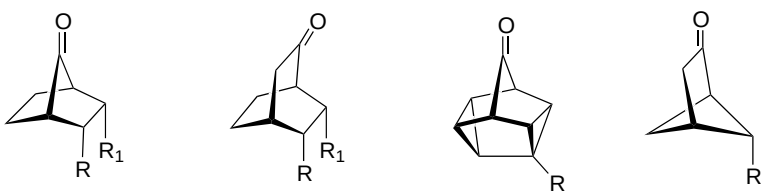

1 **2** **3** **4**

* Corresponding authors.

ever, 5-*exo*-substituted derivatives like **4** are synthetically quite inaccessible.[4] In this context, a recent report[5] on the synthesis of **4** (R = $COOCH_3$), although involving an arduous and long synthetic sequence, provided an opening. Employing this route, emanating from readily available bicyclo[2.2.1]hept-5-en-2-one, we have synthesized several 5-*exo*-bicyclo[2.1.1]hexan-2-one derivatives **4a**–**f**[6] and subjected them to hydride addition.[7]

Bicyclic ketones **4a**–**f** on reduction with sodium borohydride furnished (*E*)-**5a**–**f** and (*Z*)-**6a**–**f** alcohols in near quantitative yield (Scheme 1).[7] The observed diastereoselectivities (*E*:*Z* ratio) are displayed in Scheme 1 and were determined through GLC and ^{1}H NMR analyses. The stereostructures of **5a**–**f** and **6a**–**f** were unambiguously determined on the basis of: (i) the relative deshielding (ca. 0.45 ppm) of the H(6) *endo* protons in the (*E*)-alcohols **5a**–**f** compared to the (*Z*)-alcohols **6a**–**f**. The H(6) *endo* proton in **5a**–**f** and **6a**–**f** appeared as a diagnostic triplet ($J = \sim 7$ Hz) due to long range (4 bond) coupling with the H(5) *endo* proton and could be readily recognized; (ii) shielding (ca. 3–5 ppm) of the C(6) carbon resonance in the (*E*)-series compared to the (*Z*)-series.

The stereoselectivities during hydride reduction of **4a**–**f** are generally consistent with the trend observed earlier with related systems.[1–3] However, the *syn*-face preference of the remote electron withdrawing substituents like cyano and ester is diminished in the bicyclo[2.1.1]hexane system **4** compared to the norbornyl system **1**. The *anti*-face selectivity in the case of **4d**,**f** is contrary to the prediction based on the Cieplak model.[9] In the case of the alkyl substituted derivative **4e**, there is a marginal preference for the *anti*-face addition, see Scheme 1.

The experimental probe **4a**–**f** provided an opportunity to test the validity and predictability of the proposed computational models[3b,8] at different levels of theory. The reduced selectivities observed in the case of **4** (cf. **1**–**3**)[3a–e] were indicative of the involvement of more subtle factors and thereby this system was expected to provide a stringent test for the performance of computational techniques. While ab initio and DFT level calculations were performed using the Gaussian 94 suite of programs,[10] the MNDO[11a] and AM1[11b] calculations used the MOPAC program package. First, the economically attractive semi-empirical, MNDO and AM1 methods were employed to discern the orbital and electrostatic effects using the hydride and charge models as well as the LiH transition states (Table 1). The charge and hydride model calculations were carried out by placing a point charge and hydride ion, respectively, 1.4 Å away from the carbonyl carbon on both sides along the trajectory perpendicular to the carbonyl face, as described earlier.[3b] The LiH transition states are located on the potential energy surface and characterized as saddle points by the frequency calculations. Charge models overestimate the preference for the *anti* attack, especially at MNDO level (Table 1). However, the results of hydride and LiH transition state models

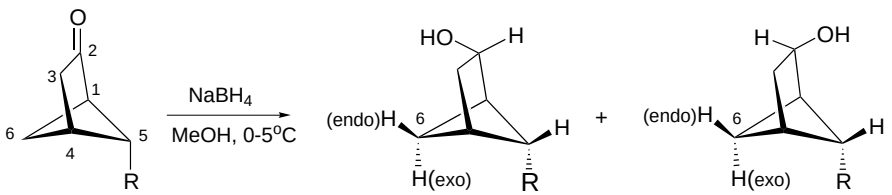

4a	R = CN	(*E*)-**5a**	75%	(*Z*)-**6a**	25%
b	R = COOMe	**b**	66%	**b**	34%
c	R = C≡CH	**c**	60%	**c**	40%
d	R = CH_2OH	**d**	48%	**d**	52%
e	R = CH_2CH_3	**e**	47%	**e**	53%
f	R = $CH{=}CH_2$	**f**	44%	**f**	56%

Scheme 1.

Table 1. The relative energy for *anti*-face addition with respect to the *syn*-face addition calculated using the hydride model, charge model and for the LiH addition transition states at MNDO and AM1 levels.[a] All values are given in kcal/mol

4. R =	Charge model		Hydride model		Transition states	
	MNDO	AM1	MNDO	AM1	MNDO	AM1
CN	−0.26	1.85	0.67	1.19	0.26	0.58
COOMe	−1.65	0.56	0.47	1.02	−0.05	0.11
CCH	−2.00	−0.37	−0.04	0.38	−0.14	0.17
CH_2OH	−3.95	−3.27	−0.63	−0.23	−0.35	−0.56
CH_2CH_3	−4.29	−3.02	−0.78	−0.41	−0.32	−0.24
$CHCH_2$	−3.06	−3.50	−0.38	−0.68	−0.24	−0.24

[a] A positive value denotes *syn* preference and a negative value denotes *anti* preference.

are in good agreement with the experimental observations.

The hydride and LiH transition state models were modelled also at ab initio and density functional theory level. Transition states are optimized (transition states for *syn* and *anti* attack in **4a** are given in Fig. 1) and characterized by frequency calculations at the B3LYP/6-31G* level, followed by single point calculations at HF and MP2 levels. Table 2 clearly indicates that the relative barrier heights are virtually insensitive to the level of theory. All methods correctly reproduce the higher *syn* selectivity for the cyano substituent, and *anti* selectivity of ethyl and hydroxymethyl groups. The success of the hydride model over the charge model in correctly reproducing the observed selectivities highlights the subtle interplay of electrostatic and orbital effects in the nucleophilic additions to the carbonyl group.

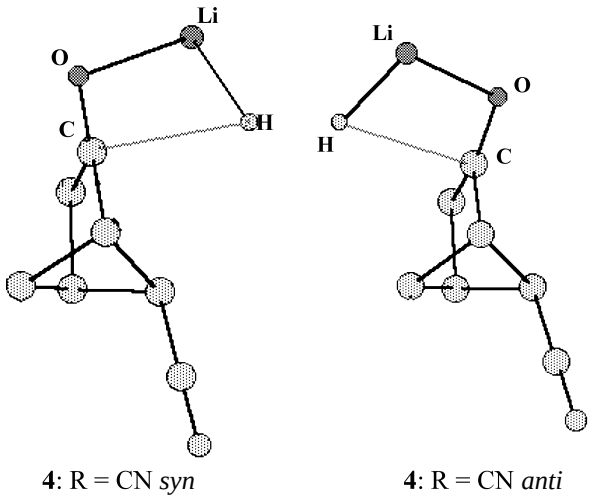

4: R = CN *syn* **4**: R = CN *anti*

Figure 1. The B3LYP/6-31G* optimized LiH addition transition state structures.

The Cieplak type hyperconjugative effects and the perturbations in carbonyl pyramidalization upon metal ion complexation[8b] are estimated by NBO analysis[12] and proton complexation models, respectively, at B3LYP/6-31G* level of theory (Table 3). The interaction energies between the σ 1,5- and σ 1,6-donors and π*CO acceptors, as obtained from the NBO second-order perturbative analysis, predict uniform preference for an *anti* attack in all cases. The metal ion complexation model predicts the preferential *syn* attack for **4a** and *anti* for **4b–f**. Also, the differences in the pyramidalization, gauged by the difference in the dihedral angles D1 and D2, do not correlate very well with the observed selectivities. Thus, the simplistic approximations in the NBO analysis and cation complexation models have rather limited predictability. In contrast, the hydride model, which takes into account electrostatic and orbital effects, seems to provide reliable and quick answers even at semi-empirical level (Table 1).

In summary, a systematic experimental and computational study on the new system **4**, ranging from semi-empirical to ab initio and DFT, indicates that the

Table 2. The relative energy for *anti*-face addition with respect to the *syn*-face addition calculated using the hydride model and for the LiH addition transition states at HF, B3LYP and MP2 levels.[a] All values are given in kcal/mol

4. R =	Hydride model			Transition state		
	B3LYP/6-31G*	HF/6-31G*[b]	MP2/6-31G*[b]	B3LYP/6-31G*	HF/6-31G*[b]	MP2/6-31G*[b]
CN	1.28	1.36	1.52	1.16	0.76	1.13
COOMe	−1.95	−0.57	−0.72	0.46	0.40	0.52
CCH	−0.15	−0.67	−0.03	0.41	0.33	0.45
CH_2OH	−1.03	−1.17	−0.78	−0.14	−0.07	−0.14
CH_2CH_3	−1.89	−2.72	−1.82	−0.09	−0.07	−0.11
$CHCH_2$	−1.46	−2.37	−1.48	0.34	0.13	0.27

[a] A positive value denotes *syn* preference and a negative value denotes *anti* preference.
[b] Single point energy calculations on B3LYP/6-31G* optimized structures.

Table 3. The NBO σ–π* interaction energy (in kcal/mol), which estimates the Cieplack-type hyperconjugative effect, and the dihedral angles which gauges carbonyl pyramidalization for the proton complex. Values in parentheses correspond to the neutral reactant. All values are at B3LYP/6-31G* on geometries optimized at the same level

4. R =	σ_{1-5}–π^*_{2-7}	σ_{1-6}–π^*_{2-7}	Δ[a]	D1[b]	D2[b]
CN	10.50 (4.73)	9.51 (4.41)	0.99 (0.32)	138.0 (135.9)	136.7 (136.3)
COOMe	11.93 (4.94)	8.81 (4.46)	3.12 (0.48)	133.4 (135.9)	141.5 (136.3)
CCH	14.53 (5.01)	7.77 (4.51)	6.76 (0.50)	132.1 (135.5)	143.3 (136.8)
CH_2OH	11.40 (4.74)	9.82 (4.80)	1.58 (−0.06)	135.0 (135.8)	139.4 (136.1)
CH_2CH_3	14.24 (4.88)	8.37 (4.78)	5.87 (0.10)	130.4 (135.1)	144.4 (136.8)
$CHCH_2$	16.01 (5.17)	7.60 (4.60)	8.41 (0.57)	130.7 (135.3)	144.8 (137.0)

[a] Δ is the difference between σ_{1-5}–π^*_{2-7} and σ_{1-6}–π^*_{2-7}.
[b] D1 and D2 are dihedral angles C_7–C_2–C_1–C_5 and C_7–C_2–C_1–C_6, respectively.

simple hydride model (as well as LiH transition state model) at semi-empirical level constitutes an economical predictive tool for facial selectivities in nucleophilic additions to sterically unbiased ketones and reinforces our earlier[3b] proposals in this regard.

Acknowledgements

R.S., U.D.P. and V.G. thank CSIR, UGC and JNCASR, respectively, for research fellowships.

References

1. For recent reviews on diastereoselection, see a thematic issue: *Chem. Rev*. **1999**, *99*, 1069–1480; (b) Mehta, G.; Chandrasekhar, J. *Chem. Rev*. **1999**, *99*, 1437.
2. Mehta, G.; Khan, F. A. *Tetrahedron Lett*. **1992**, *33*, 3065.
3. (a) Mehta, G.; Khan, F. A. *J. Am. Chem. Soc*. **1990**, *112*, 6140; (b) Ganguly, B.; Chandrasekhar, J.; Khan, F. A.; Mehta, G. *J. Org. Chem*. **1993**, *58*, 1734; (c) Mehta, G.; Khan, F. A.; Ganguly, B.; Chandrasekhar, J. *J. Chem. Soc., Chem. Commun*. **1992**, 1711; (d) Mehta, G.; Ravikrishna, C.; Ganguly, B.; Chandrasekhar, J. *J. Chem. Soc., Chem. Commun*. **1997**, 75; (e) Mehta, G.; Ravikrishna, C.; Kalyanraman, P.; Chandrasekhar, J. *J. Chem. Soc., Perkin Trans. 1* **1998**, 1895; (f) Halterman, R. L.; McEvoy, M. A. *J. Am. Chem. Soc*. **1990**, *112*, 6690; (g) Ohwada, T. *J. Am. Chem. Soc*. **1992**, *114*, 8818; (h) Wipf, P.; Kim, Y. *J. Am. Chem. Soc*. **1994**, *116*, 117678; (i) Fraser, R. R.; Faibish, N. C.; Kong, F.; Bednarski, F. *J. Org. Chem*. **1997**, *62*, 6164; (j) Li, H.; le Noble, W. J. *Recl. Trav. Chim. Pays-Bas* **1992**, *111*, 199.
4. (a) Meinwald, J.; Crandall, J. K. *J. Am. Chem. Soc*. **1966**, *88*, 1292; (b) Wiberg, K. B.; Ubersax, R. W. *J. Org. Chem*. **1972**, *37*, 3827.
5. Conti, P.; Kozikowski, A. P. *Tetrahedron Lett*. **2000**, *41*, 4053.
6. Substrates **4a** and **4c**–**f** were prepared from carbonyl protected **4b**[5] through routine but non-trivial functional group transformations and overall access to **4a**–**f** was certainly a very demanding endeavor.
7. All new compounds reported here were fully characterized on the basis of complementary spectroscopic (IR, ^{1}H and ^{13}C NMR and MS) and analytical data. Except in the case of **5c**/**6c** and **5e**/**6e**, the diastereomers **5a**,**b**,**d**,**f** and **6a**,**b**,**d**,**f** were separated and individually characterized. Selected spectral data: ^{13}C NMR δ (75 MHz, $CDCl_3$); **5a**: 120.5, 70.1, 50.1, 43.7, 38.3, 37.3, 33.7. **6a**: 121.7, 70.8, 51.0, 43.7, 37.8, 37.4, 35.4. **5b**: 173.0, 71.4, 54.0, 51.7, 49.3, 42.2, 38.7, 33.3. **6b**: 174.3, 72.0, 51.7, 50.7, 49.8, 42.4, 38.6, 37.7. **5c**/**6c**: 100.6, 84.8, 71.8, 71.1, 68.7, 52.1, 51.6, 44.7, 44.6, 40.9, 38.2, 37.5, 37.3, 33.1, 29.7. **5d**: 72.3, 61.0, 54.3, 46.9, 39.6, 39.4, 32.0. **6d**: 72.4, 61.4, 50.1, 47.0, 39.5, 39.4, 36.4. **5e**/**6e**: 72.9, 72.5, 54.3, 49.7, 48.8, 48.7, 41.0, 40.9, 39.9, 39.8, 36.4, 31.8, 20.1, 19.9, 13.5, 13.2. **5f**: 136.9, 115.8, 72.1, 55.6, 50.1, 42.6, 39.3, 31.8. **6f**: 137.4, 116.1, 72.7, 51.5, 50.3, 42.8, 39.3, 36.4.
8. (a) Paddow-Row, M. N.; Wu, Y.-D.; Houk, K. N. *J. Am. Chem. Soc*. **1992**, *114*, 10638; (b) Jeyaraj, D.; Yadav, A. A.; Yadav, V. K. *Tetrahedron Lett*. **1997**, *38*, 4483.
9. Cieplack, A. S. *J. Am. Chem. Soc*. **1981**, *103*, 4540.
10. Frisch, M. J.; Trucks, G. W.; Schlegel, H. B.; Jones, P. M. W.; Johnson, B. G.; Robb, M. A.; Cheeseman, J. R.; Kheith, T.; Petersson, G. A.; Montgomery, J. A.; Gaghavachari, M. A.; Al-Laham, M. A.; Zakrzewski, V. G.; Ortiz, J. V.; Foresman, J. B.; Cioslowski, J.; Stefanov, B. B.; Nanayakkara, A.; Challacombe, M.; Peng, C. Y.; Ayala, P. Y.; Chen, W.; Wong, M. W.; Andres, J. L.; Replogle, E. S.; Gomperts, R.; Martin, R. L.; Fox, D. J.; Binkley, J. S.; Defrees, D. J.; Baker, J.; Stewart, J. P.; Head-Gordon, M.; Gonzalez, C.; Pople, J. A. Gaussian 94: Gaussian, Inc., Pittsburgh, PA, 1995.
11. (a) Dewar, M. J. S.; Theil, W. *J. Am. Chem. Soc*. **1977**, *99*, 4899; (b) Dewar, M. J. S.; Zoebisch, Z.; Healy, E. F.; Stewart, J. J. P. *J. Am. Chem. Soc*. **1985**, *107*, 3902.
12. NBO Version 3.1. Glendening, E. D.; Reed, A.; Carpenter, E J. E.; Weinhold, F.